

Layer by Layer: Uncovering Where Multi-Task Learning Happens in Instruction-Tuned Large Language Models

Anonymous ACL submission

Abstract

Fine-tuning pre-trained large language models (LLMs) on a diverse array of tasks has become a common approach for building models that can solve various natural language processing (NLP) tasks. However, where and to what extent these models retain task-specific knowledge remains largely unexplored. This study investigates the task-specific information encoded in pre-trained LLMs and the effects of instruction tuning on their representations across a diverse set of over 60 NLP tasks. We use a set of matrix analysis tools to examine the differences between the way pre-trained and instruction-tuned LLMs store task-specific information. Our findings reveal that while some tasks are already encoded within the pre-trained LLMs, others greatly benefit from instruction tuning. Additionally, we pinpointed the layers in which the model transitions from high-level general representations to more task-oriented representations. This finding extends our understanding of the governing mechanisms of LLMs and facilitates future research in the fields of parameter-efficient transfer learning and multi-task learning.¹

1 Introduction

While pre-trained LLMs exhibit impressive performance across diverse tasks and demonstrate remarkable generalization capabilities (Brown et al., 2020; Wei et al., 2022b; Touvron et al., 2023; Chowdhery et al., 2023; OpenAI et al., 2024), the representations they learn and the task-specific information encoded during pre-training remain largely opaque and unexplored.

Recent research has investigated fine-tuning strategies to adapt LLMs to specific tasks, including supervised fine-tuning on task-specific datasets and instruction tuning (Mishra et al., 2022; Chung

¹We will make our code and data publicly available upon acceptance.

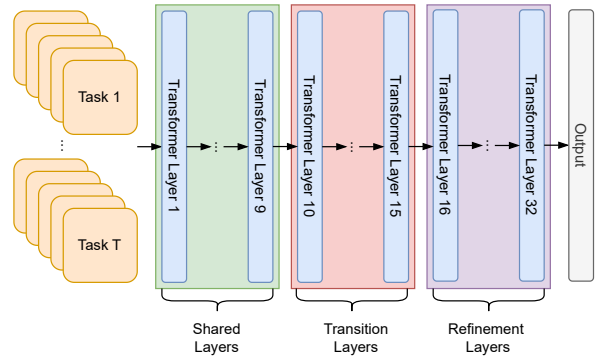


Figure 1: An illustration of our findings using the Llama 2 7B model (Touvron et al., 2023) as an example. We show that when instruction tuning on T different tasks, the layers are divided into three functional sections: the shared layers (layers 1 to 10) form general representations shared among all tasks, the transition layers (layers 10 to 15) transition the representations into task-specific information, and the refinement layers (layers 16 to 32) continue to refine the representations toward specific tasks.

et al., 2022; Sanh et al., 2022). While these approaches have shown promising results in tailoring LLMs for improved task performance, a comprehensive understanding of their impact on the learned representations is still lacking.

In this study, we perform a set of analyses to investigate task-specific information encoded in pre-trained LLMs and the effects of instruction tuning on their representations. The analysis leverages a sub-population analysis technique called Model-Oriented Sub-population and Spectral Analysis (MOSSA; Zhao et al. 2022), which provides an alternative to traditional probing methods for analyzing model representations within specific sub-populations of the training data. MOSSA involves comparing two models: a *control* model trained on the data relevant to the sub-population of interest (e.g., a particular task), and an *experimental* model that is identical to the control model but is also trained on additional data from different

sources (e.g., multiple tasks). By analyzing the representational differences between these models, we can isolate the task-specific information encoded within the control model for the sub-population of interest.

To compare the representations learned by different LLM variants, we leverage the Center Kernel Alignment (CKA; Kornblith et al., 2019) metric. CKA measures the alignment between representations in a kernel space, providing a robust measure of similarity that is insensitive to scaling and centering. By using MOSSA and CKA, we investigate the following research questions:

1. To what extent are different NLP tasks already encoded in pre-trained LLMs?
2. In what ways does instruction tuning modify the representational landscape of LLMs?
3. Do the representational effects of instruction tuning generalize to unseen tasks?

Through an extensive analysis spanning over 60 diverse NLP tasks following the Flan framework (Longpre et al., 2023), we shed light on the underlying mechanisms that govern the encoding and adaptation of task-specific information within LLMs under instruction tuning. A key finding of our work is the identification of three functional groups of layers: a) shared layers, in which more general information is learned and shared across tasks; b) transition layers, in which task-specific information is intensified; c) refinement layers, in which the LLMs continue to refine their representations towards task-specific predictions. Our findings contribute to a deeper understanding of the inner workings of LLMs and hold promising implications for future research in parameter-efficient fine-tuning (PEFT), multi-task learning (MTL), and model compression, benefiting a wide range of NLP applications.

We structure this study as follows: §2 describes our methodology for our analysis, while §3 outlines the experimental setup and tools used to train and analyze our LLMs. §4 then attempts to answer each of the research questions outlined above by presenting and analyzing our results. Finally, in §5, we summarize our key findings and discuss their potential implications.

2 Methodology

We leverage the MOSSA framework introduced by Zhao et al. (2022). Unlike standard probing meth-

ods (Belinkov et al., 2017a,b; Giulianelli et al., 2018), which build a model to predict a downstream task for quantifying encoded information, MOSSA compares representations from two models: a control model trained on data of interest and an experimental model trained on additional data from different sources. Here, the data of interest refers to tasks. Probing methods, while useful, can be limited because they rely on different metrics to evaluate performance across various tasks, making it challenging to directly compare the amount of information stored about tasks as diverse as sentiment analysis and translation. MOSSA, on the other hand, circumvents this issue by comparing the latent representations of models rather than their downstream performance metrics. MOSSA calculates the similarity between the representations of the control and experimental models, thus representing the information captured from the relevant sub-population of data through their latent representations. By comparing different models to each other, we can learn what information is captured when a subset of the data is used versus the whole dataset.

We use matrix analysis to compare representation similarity between the experimental model, such as pre-trained, instruction-tuned, and corresponding single-task control models trained on individual tasks. Intuitively, a high similarity between the experimental and control models indicates the experimental model stores task-specific information learned by the control model, which was fine-tuned solely on data from that task. The similarity is measured using the CKA metric, which quantifies the similarity between two representations in a kernel space.

Formally, let $[T]$ be an index set of tasks, and let \mathbf{E} be the experimental model and \mathbf{C}_t be the control model for task $t \in [T]$. We assume a set of inputs $\mathcal{X} = \bigcup_{t=1}^T \mathcal{X}_t$, where each $\mathcal{X}_t = \{\mathbf{x}_{t,1}, \dots, \mathbf{x}_{t,n}\}$ represents a set of input instructions for task t . For simplicity, we assume that all sets have the same size n , although this is not a strict requirement.

For each $t \in [T]$ and $i \in [n]$, we apply the experimental model \mathbf{E} and the control model \mathbf{C}_t to the input instruction $\mathbf{x}_{t,i}$ to obtain two corresponding representations $\mathbf{y}_{t,i} \in \mathbb{R}^d$ and $\mathbf{z}_{t,i} \in \mathbb{R}^{d_t}$, respectively. Here, d is the dimension of the experimental model’s representations, and d_t is the dimension of the control model representations for task t . To obtain the representations $\mathbf{y}_{t,i}$ and $\mathbf{z}_{t,i}$, we use the last token’s representation following previous work

(Qiu et al., 2024; Wang et al., 2024), as LLMs are decoder-only and the last token captures all input information. These representations can be extracted from any layers of the respective models.

By stacking these vectors into two matrices for each task t , we obtain the paired matrices $\mathbf{Y}_t \in \mathbb{R}^{n \times d}$ and $\mathbf{Z}_t \in \mathbb{R}^{n \times d_t}$. We calculate the CKA value between \mathbf{Y}_t and \mathbf{Z}_t following the procedure:

- Computing the kernel matrices $K_{\mathbf{Y}_t} \in \mathbb{R}^{n \times n}$ and $K_{\mathbf{Z}_t} \in \mathbb{R}^{n \times n}$ for \mathbf{Y}_t and \mathbf{Z}_t , respectively, using the same kernel function (e.g., linear, Gaussian, or polynomial).²
- Centering the kernel matrices by $\tilde{K}_{\mathbf{Y}_t} = K_{\mathbf{Y}_t} - \frac{1}{n}\mathbf{1}K_{\mathbf{Y}_t} - \frac{1}{n}K_{\mathbf{Y}_t}\mathbf{1} + \frac{1}{n^2}\mathbf{1}K_{\mathbf{Y}_t}\mathbf{1}$, similarly for $\tilde{K}_{\mathbf{Z}_t}$, where $\mathbf{1}$ is a matrix of ones.
- Computing the CKA value by first compute the Frobenius inner product of the centered Gram matrices: $\text{HSIC}(K_{\mathbf{Y}_t}, K_{\mathbf{Z}_t}) = \text{Tr}(\tilde{K}_{\mathbf{Y}_t}^\top \tilde{K}_{\mathbf{Z}_t})$, where Tr denotes the trace of a matrix. Then normalize the CKA value:

$$\text{CKA}(\mathbf{Y}_t, \mathbf{Z}_t) = \frac{\text{HSIC}(K_{\mathbf{Y}_t}, K_{\mathbf{Z}_t})}{\sqrt{\text{HSIC}(K_{\mathbf{Y}_t}, K_{\mathbf{Y}_t}) \cdot \text{HSIC}(K_{\mathbf{Z}_t}, K_{\mathbf{Z}_t})}}. \quad (1)$$

While other similarity metrics like SVCCA (Raghu et al., 2017) exist, they have a limitation due to the constraint of being invariant to invertible linear transformations, which requires the number of data points to be greater than the number of representation dimensions. We use CKA as it has shown robust results when the data sample is smaller (Kornblith et al., 2019), as is sometimes the case for datasets used in our work.

Our method provides an approach to quantify the task-specific information encoded in the representations of LLMs. By comparing the experimental model’s representations with those of single-task control models, we can gain insights into the extent to which the experimental model captures task-specific knowledge and how this knowledge is distributed across its representations.

3 Experimental Setup

Data We use the Flan 2021 dataset (Wei et al., 2022a) to fine-tune our LLMs. The Flan dataset is a comprehensive collection of more than 60 NLP datasets, including both language understanding and generation tasks. These datasets are organized into twelve task clusters, where datasets within a

²For linear kernel, which is what we use in our experiment, $K_{\mathbf{Y}_t} = \mathbf{Y}_t \mathbf{Y}_t^\top$, and $K_{\mathbf{Z}_t} = \mathbf{Z}_t \mathbf{Z}_t^\top$.

given cluster belong to the same task type. To enhance instruction diversity, we follow the approach of Wei et al. (2022a) and use ten unique natural language instruction templates for each dataset. These templates provide varying descriptions of the task to be performed. Our instruction tuning pipeline combines all datasets and randomly samples from each dataset during training. To mitigate the impact of dataset size imbalances, we limit the number of training examples per task cluster to 50k and use the examples-proportional mixing scheme (Raffel et al., 2020) with a mixing rate maximum of 3,000 per task. This means that no task receives additional sampling weight for examples in excess of 3,000. We provide further details about the dataset in Appendix A.

Models We have two types of models: the experimental model \mathbf{E} , fine-tuned using all T available tasks, and the single-task model \mathbf{C}_t for $t \in [T]$, fine-tuned only on the t -th task. In some experiments, the model \mathbf{E} can also be the pre-trained model. We use the Llama 2 models (Touvron et al., 2023) as the starting training checkpoint for both \mathbf{E} and \mathbf{C}_t . Specifically, we use the 7B variant, which consists of 32 layers and 4096 hidden dimensions.

Training We use LoRA (Hu et al., 2022) for fine-tuning our LLMs, with the rank r set to 8. We use the AdamW optimizer (Loshchilov and Hutter, 2019) with a learning rate of 5×10^{-5} for fine-tuning the instruction dataset. We use the same vocabulary, tokenizer, and learning rate scheduler for Llama 2-7B as in Touvron et al. (2023). We train the multi-task model \mathbf{E} (which we refer to as Llama 2-SFT in our experiment) for a maximum of 100K steps and the single-task models \mathbf{C}_t for a maximum of 10K steps, using validation set cross-entropy loss for early stopping. Our multi-task models are trained on four NVIDIA A100 GPUs with a batch size of 16 per GPU, while single-task models are trained on one NVIDIA A100 GPU with a batch size of 16. We use PyTorch (Paszke et al., 2019), the HuggingFace library (Wolf et al., 2020), and the LLaMA-Factory library (Zheng et al., 2024) for all model implementations and LoRA fine-tuning.

4 Experiments and Results

To shed light on the underlying mechanisms of MTL (Caruana, 1997) in LLMs, we start by examining what NLP tasks are encoded in the pre-trained LLM representations, establishing a base-

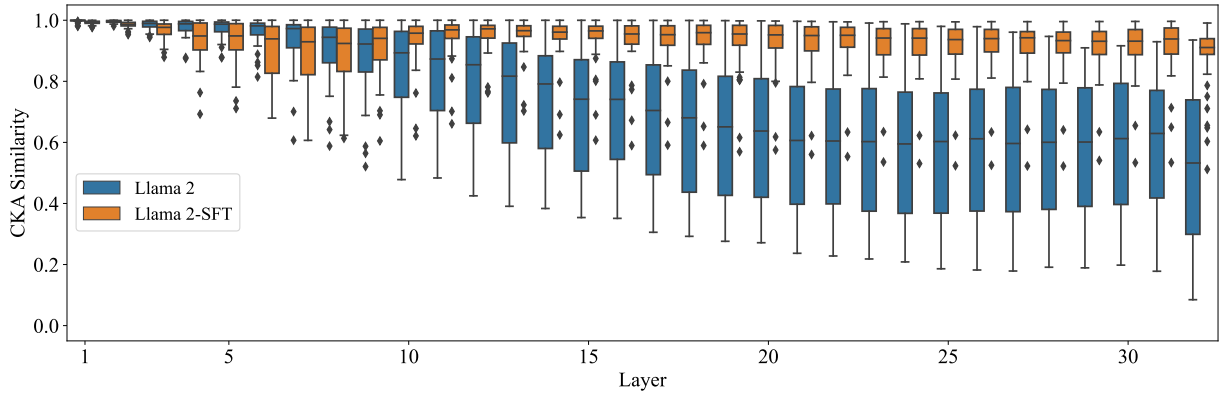


Figure 2: Distribution of CKA similarities across all layers for the pre-trained Llama 2 model and the instruction-tuned Llama 2-SFT model. The boxplots illustrate the spread and variation of CKA similarities between each model and the control models across different tasks. The comparison between the two models highlights the impact of instruction tuning on shaping task-specific representations in different layers.

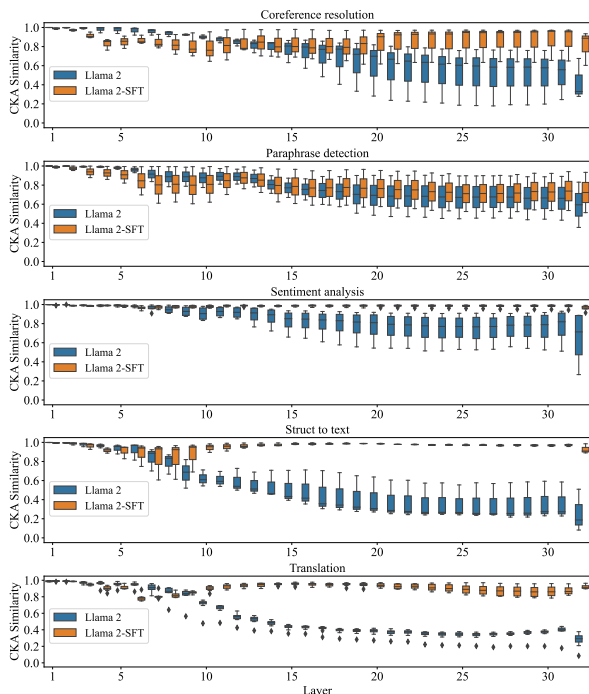


Figure 3: Distribution of CKA similarities across all layers for the pre-trained Llama 2 model and the instruction-tuned Llama 2-SFT model, grouped by different task clusters.

line for comparison with the instruction-tuned model (§4.1). Then, using matrix analysis methods, we contrast the representational properties of the pre-trained and instruction-tuned LLMs to understand the effects of instruction tuning (§4.2, 4.3, and 4.4). Finally, we evaluate the generalization of our findings to unseen tasks (§4.5).

4.1 Task Information in Pre-trained LLMs

To identify task-relevant information in pre-trained LLMs, we compared representations from the pre-

trained Llama 2 model with task-specific fine-tuned models ($\{C_t\}_t$). Figure 2 shows the distribution of CKA similarities across all tasks and layers for the Llama 2 model. The CKA similarities between pre-trained Llama 2 and control models generally decrease through higher layers.

Llama 2 maintains high CKA similarities in earlier layers, and since CKA compares against control models fine-tuned on individual tasks, this suggests that representational changes in the earlier layers are minimal across tasks. However, we observe widespread variance in CKA values across different tasks in the middle and higher layers, suggesting that some tasks are better captured in the Llama 2 model representations than others.

To gain a more fine-grained understanding, we analyzed the CKA results at the task cluster level, where each cluster consists of a group of similar tasks. The Flan dataset organizes tasks into 12 different clusters, detailed in Appendix A. We present CKA results for a selection of representative clusters in Figures 3, with the full results provided in Appendix B.2.

For clusters like closed-book QA, commonsense reasoning, paraphrase detection, and sentiment analysis, which heavily rely on general linguistic and semantic understanding, the CKA similarity for Llama 2 is high. This indicates that pre-trained models already encode these tasks well in their representations. Conversely, for clusters like coreference resolution, reading comprehension, structured data to text generation, summarization, and translation, which require specialized, structured, or domain-specific knowledge involving complex transformations or extended context management,

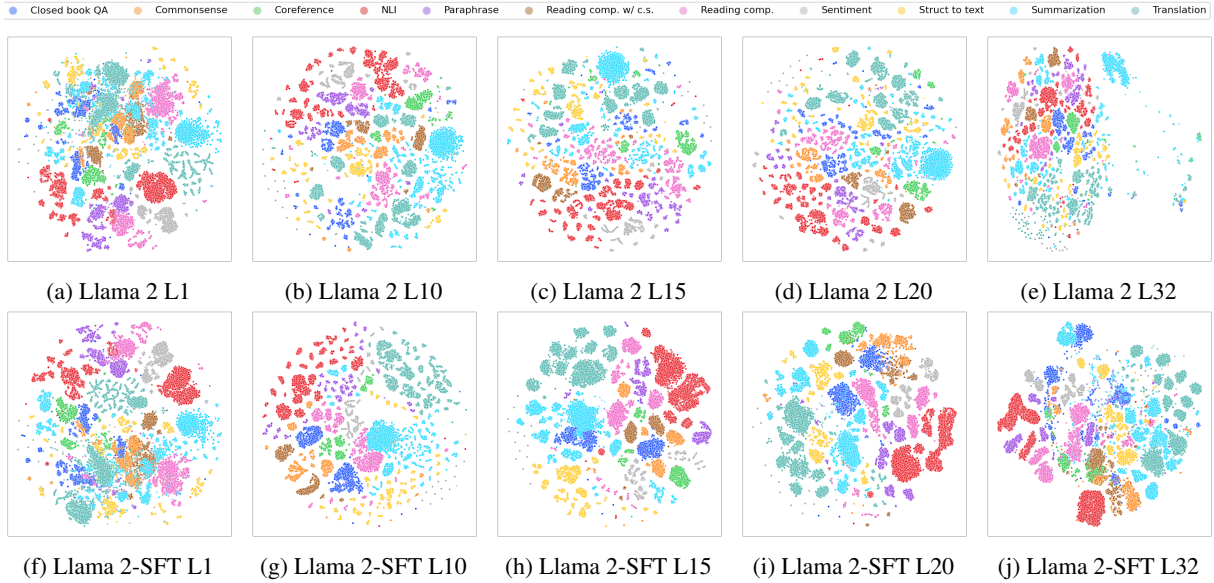


Figure 4: t-SNE visualizations of the representations for each task cluster in different layers of the pre-trained Llama 2 model and the instruction-tuned Llama 2-SFT model. Each subplot presents the t-SNE projection of the representations, color-coded by task cluster, for a specific layer of the respective model. “Reading comp.” denotes reading comprehension tasks, and “reading comp. w/ c.s.” denotes reading comprehension tasks with commonsense reasoning.

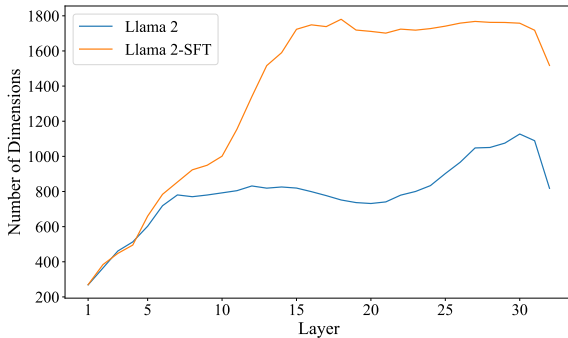


Figure 5: Average number of dimensions required to explain 99% of the representational variance across all tasks, as a function of the layer number.

the CKA similarities are low, suggesting that next token prediction at pre-training is insufficient for encoding these tasks.

4.2 Impact of Instruction Tuning

Mapping Layers to Their Functionality To investigate how instruction tuning affects the representations learned by LLMs, we compared the instruction-tuned model (Llama 2-SFT) with task-specific fine-tuned control models. As illustrated in Figure 2, the CKA similarities between Llama 2-SFT and the control models do not decrease as significantly as those for the pre-trained model (Llama 2) across layers. In the early layers (1 to 9), we ob-

serve that for many tasks, the CKA scores are lower for Llama 2-SFT compared to Llama 2, indicating that Llama 2-SFT representations diverge from those of the control models, which were fine-tuned on individual tasks (thus specializing in them). This suggests that, unlike the Llama 2 model, training Llama 2-SFT on a high number of tasks encourages it to diverge from the control models’ representations and learn more general representations in the lower layers, a characteristic typical of MTL models. We denote layers 1-9 as “shared layers”, as our findings suggest their representations are shared across tasks, similar to more studied MTL models.

In the middle layers (10-15), there is a significant transition, with the Llama 2-SFT model exhibiting high similarity to *all control models*. This indicates that these layers encode a high degree of task-specific information, as their representations are almost identical to those of the specialized control models. We denote layers 10-15 as “transitional layers”, as our findings suggest the transition to task-specific representations occurs within these layers. This trend continues, albeit to a lesser extent, up to the final layers (16-32), which we denote as “refinement layers”, as they keep refining the representations up to the final prediction. Based on our findings, we can map each layer in the Llama 2-SFT model to its corresponding function with respect to MTL (see Figure 1). While previous work

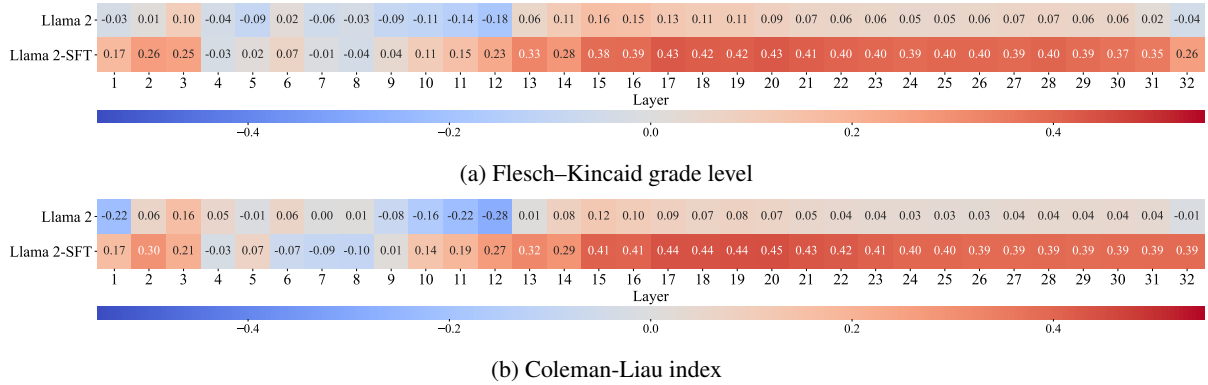


Figure 6: Pearson correlation results between the CKA similarities for all tasks and their reading difficulty among all layers. Higher values in reading difficulty measures correspond to greater reading difficulty.

(Wei et al., 2022a; Chung et al., 2022) has empirically demonstrated the effectiveness of instruction tuning for improving performance on a variety of NLP tasks, to the best of our knowledge, we are the first to propose such a mapping. In the following sections, we provide additional analyses to further validate our mapping.

Examining individual task clusters Figures 3 demonstrates that for tasks that are not well encoded in the pre-trained Llama 2 (e.g., structured data to text generation, translation), the CKA similarities from the instruction-tuned Llama 2-SFT remained high throughout all transition and refinement layers (10-32). Instruction tuning for these tasks induced significant representational shifts, adapting the model’s internal structure to meet their specific demands. This aligns with prior work (Aghajanyan et al., 2021) showing that tasks requiring more sophisticated reasoning and modeling benefit greatly from task-specific tuning of pre-trained language models.

4.3 Representation Clustering and Variance Analysis

To further investigate representational differences, we used t-SNE (Van der Maaten and Hinton, 2008) to visualize task clusters across layers. Figure 4 presents a representative selection of layers, including a shared layer (layer 1), transition layers (layers 10 and 15), and refinement layers (layers 20 and 32). The full results for all layers are provided in Appendix B.2. In the first layer, both Llama 2 and Llama 2-SFT exhibit similar clustering. However, as we move to the transition layers, from layers 10 to 15, the Llama 2-SFT model forms more distinct task clusters compared to the Llama

2 model. This is further evidence that instruction tuning transforms the representations towards task-specificity in the transition layers. This clustering becomes increasingly pronounced in refinement layers, highlighting the effectiveness of instruction tuning in differentiating task-specific information and enhancing the ability to specialize representations for different tasks.

To quantify these differences, we performed variance analysis on the representations. We sought to determine if the model’s ability to retain a large amount of task-specific information for many tasks affects its representation complexity. We analyzed the number of principal components required to explain 99% of the variance in representation matrices across layers. The average number of components over all tasks is presented in Figure 5. In the shared layers, both Llama 2 and Llama 2-SFT models require a similar number of dimensions. Then, in the transition layers, Llama 2-SFT model begins to require more dimensions, suggesting it captures more complex task-specific information. This further demonstrates that the transition layers are indeed the layers where the transition to the task-specific representations occurs.

4.4 Assessing Task Specific Information via Readability

In the preceding sections, we observed that the Llama 2 model exhibited a high variance in the amount of task-specific information stored across different tasks. In contrast, the Llama 2-SFT model demonstrated a low variance, storing a high level of task-specific information in its transition and refinement layers. While the Llama 2-SFT model exhibited low variance, we aimed to investigate the task priorities within the representation and identify

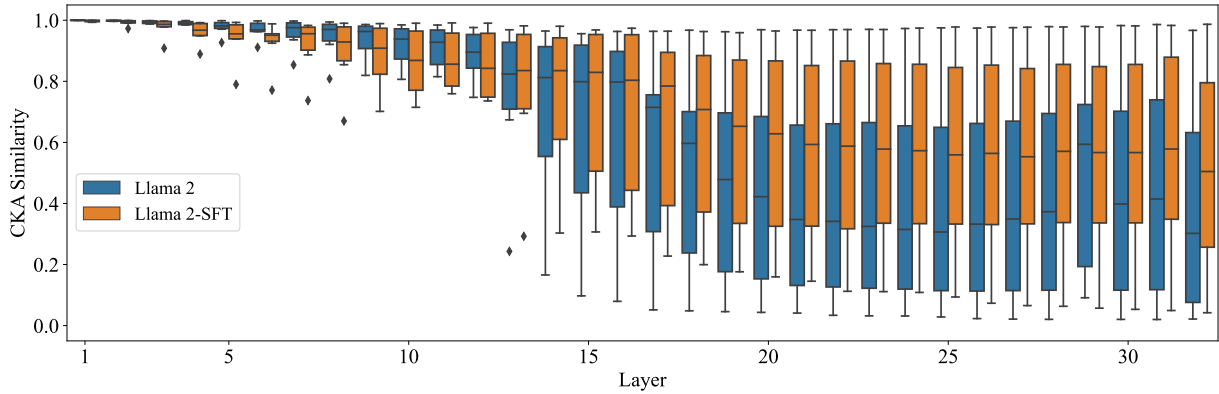


Figure 7: Distribution of CKA similarities across all layers for the pre-trained Llama 2 model and the instruction-tuned Llama 2-SFT model on unseen tasks.

features that could predict it. Previous research by Zhao et al. (2022) has shown that when masked language models, such as BERT (Devlin et al., 2019), are trained on data from multiple domains, they tend to allocate their parameters to store domain-specific information. Unlike our approach, which examines instruction-level representations using the last token of an instruction, their study used the MOSSA method to analyze contextualized word embeddings, allowing them to focus on domain-specific words. We followed a similar analysis to examine task-specific information, which is strongly related to domain-specific information (as tasks can be viewed as domains). We used readability as a proxy for domain-specific information, relying on the finding by Pitler and Nenkova (2008) that texts with more domain-specific and less commonly used words tend to have lower readability, resulting in higher reading difficulty scores.

We used two highly popular reading difficulty measures: the Flesch-Kincaid grade level score (Kincaid et al., 1975) and the Coleman-Liau Index (Coleman and Liau, 1975). The Flesch-Kincaid score assesses text readability based on factors like average sentence length and syllables per word, with lower scores indicating easier reading. Similarly, the Coleman-Liau Index estimates the required reading grade level based on characters, words, and sentences, with higher values corresponding to greater difficulty. We conducted Pearson correlation analyses between CKA similarity and reading difficulty measures for all tasks across all layers. As illustrated in Figure 6a, we found a positive correlation between CKA similarity and the Flesch-Kincaid score for Llama 2-SFT. This correlation rapidly increases between layer 10 and layer 15 (the transition layers) and then saturates.

These transitional layers are where task specialization transformations occur, as discussed earlier. This correlation is much weaker for the Llama 2 model. A similar pattern is observed with the Coleman-Liau Index, as shown in Figure 6b. These findings suggest that instruction-tuned models encode more information for tasks with more task-specific vocabulary, as measured by their texts’ readability indices. These findings thus suggest that instruction-tuned models encode and preserve task-specific information in the transition layers and retain it through the refinement layers, complementing our earlier findings. Moreover, we previously noted that one of the advantages of CKA, compared to other similarity metrics, is its minimal requirement for a large number of data points in the analysis. To verify this, we conducted a correlation analysis between data size and CKA similarity, with the results presented in Figure 10 in Appendix B.2. The analysis revealed no clear correlation between data size and CKA similarities, indicating that the number of data points used for CKA per task does not impact the CKA similarity.

4.5 Evaluating Representations on Unseen Tasks

While our previous analyses focused on evaluating representations against models trained on the same task data, it is crucial to examine how well our findings generalize to unseen tasks. To investigate this, we held out a set of seven tasks, including conversational question answering, question classification, math problems, linguistic acceptability, and word sense disambiguation (details in Appendix A). Our instruction-tuned models had no exposure to any of these seven tasks during training.

The CKA similarity results in Figure 7 reveal an

interesting pattern. For the lower layers (up to layer 12), the Llama 2 model exhibited slightly higher CKA similarities than Llama 2-SFT for several tasks, similar to what we find in §4.2. This indicates that while the Llama 2-SFT model was not trained using these tasks, it produced more divergent representations in lower layers and thus more general than the ones produced by Llama 2 (we refer the reader to shared layers discussion in §4.2 for more details). However, as we move to the middle and higher layers responsible for encoding more specialized, task-specific knowledge, the Llama 2-SFT model began matching and ultimately surpassing the CKA similarities of the Llama 2 model. We can also see high variances between task similarities for both models, showing that we can not identify transition layers for Llama 2-SFT in this setup, just shared and refinement layers. These findings suggest that in addition to being trained on instructions, instruction-tuned models benefit from more general and thus better feature representations in their lower layers, which boost their performance for unseen instruction-based tasks compared to pre-trained LLMs.

5 Discussion

Our study offers comprehensive insights into the impact of instruction tuning on the representations learned by LLMs. Previous work has discussed the benefits of instruction tuning (Wei et al., 2022b; Chung et al., 2022; Longpre et al., 2023), but ours is the first to analyze their effects from a representational perspective.

Our analysis revealed that LLMs instruction-tuned on multiple tasks learned different representations in the lower layers compared to LLMs tuned on individual tasks. Similar to MTL, such representations can be shared and leveraged across tasks (Maurer et al., 2016). Our analysis uncovered a key novel finding – we observed clear differences between pre-trained and instruction-tuned models, with the most significant representational transformations occurring in the middle transitional layers. This finding highlights the critical role of middle layers in encoding the specialized task knowledge induced by instruction tuning. Similarly, previous studies in multilingual settings have also identified language-neutral transformations in the middle layers of the network (Muller et al., 2021; Zhao et al., 2023). Furthermore, our analysis suggests that in the refinement layers, instruction-tuned mod-

els continue to shape representations toward specific tasks but without substantial representational changes with respect to task-specific information. Overall, our finding about functionality for different layers in LLMs generally aligns with previous findings on BERT, which have shown that lower layers are more general, while upper layers are known to be more task-specific (Rogers et al., 2020; Merchant et al., 2020).

Our correlation analysis also revealed insights into the relationship between representations and task complexity. Instruction-tuned models exhibited a positive correlation with reading complexity measures in the transition and refinement layers, suggesting better encoding of task-specific information for tasks with more specific vocabulary – a capability not observed in pre-trained models. Notably, instruction tuning enabled models to preserve and enhance task-specific information across a broader range of layers, as evidenced by higher CKA similarities compared to control models. Our evaluation of unseen tasks further underscored the benefits of instruction tuning for improving generalization, with instruction-tuned models outperforming their pre-trained counterparts in deeper layers responsible for encoding complex task knowledge. This aligns with empirical evidence from Wei et al. (2022a) but also highlights how representational changes facilitated by instruction tuning strengthen cross-task transfer capabilities.

6 Conclusion

Our study used several analyses to investigate how instruction tuning shapes representations in LLMs. These analyses revealed that unlike the pre-trained LLM (Llama 2), the instruction-tuned model (Llama 2-SFT) retained a high amount of task-specific information for all tasks from the middle layers onward. Moreover, we were able to map the layers of Llama 2-SFT into three groups based on their functionality: shared layers (layers 1-9), transition layers (10-15), and refinement layers (16-32). In addition to expanding our understanding of LLMs, such mapping can greatly benefit future research in the fields of PEFT, MTL, and model compression. We also demonstrated that our mapping does not generalize to unseen tasks, revealing that a potential additional reason for the strong generalization capabilities of instruction-tuned models to unseen tasks can be related to their multi-task nature of producing more general representations.

585 Limitations

586 While our study provides valuable insights into the
587 impact of instruction tuning on the representations
588 learned by LLMs, there are several limitations that
589 should be considered.

590 Firstly, the instruction tuning in our experiments
591 was implemented using LoRA instead of full fine-
592 tuning. While LoRA is computationally efficient
593 and effective in many scenarios, it may not capture
594 the full range of representational changes that full
595 fine-tuning can achieve. This limitation might have
596 influenced the depth of insights into how instruc-
597 tion tuning affects the model representations.

598 Secondly, our study exclusively used the Llama
599 2 model due to limited computational resources
600 available. Although Llama 2 is a powerful and
601 widely used LLM, relying on a single model limits
602 the generalizability of our findings. Different mod-
603 els may exhibit varied representational dynamics
604 and responses to instruction tuning. Expanding our
605 analysis to include multiple models from different
606 architectures would provide a more comprehensive
607 understanding of these effects.

608 Additionally, we conducted our experiments on
609 the 7B parameter version of Llama 2. While this
610 model size is substantial, it is not the largest avail-
611 able. Larger models, with their greater capacity and
612 potentially different representational capabilities,
613 might show different patterns in response to fine-
614 tuning. Investigating multiple model sizes would
615 help ascertain whether the observed trends hold
616 across different scales.

617 Moreover, our experiments focused solely on
618 NLP tasks and did not explore fine-tuning on code
619 or other specialized domains. Coding tasks of-
620 ten involve unique representational challenges and
621 might reveal different insights into the impact of
622 fine-tuning. Including such tasks in future work
623 would broaden the scope and applicability of our
624 findings.

625 References

626 Armen Aghajanyan, Ankit Gupta, Akshat Shrivastava,
627 Xilun Chen, Luke Zettlemoyer, and Sonal Gupta.
628 2021. [Muppet: Massive multi-task representations
629 with pre-finetuning](#). In *Proceedings of the 2021 Con-
630 ference on Empirical Methods in Natural Language
631 Processing*, pages 5799–5811, Online and Punta
632 Cana, Dominican Republic. Association for Com-
633 putational Linguistics.

634 Yonatan Belinkov, Nadir Durrani, Fahim Dalvi, Hassan

Sajjad, and James Glass. 2017a. [What do neural
machine translation models learn about morphology?](#)
In *Proceedings of the 55th Annual Meeting of the
Association for Computational Linguistics (Volume
1: Long Papers)*, pages 861–872, Vancouver, Canada.
Association for Computational Linguistics.

Yonatan Belinkov, Lluís Màrquez, Hassan Sajjad, Nadir
Durrani, Fahim Dalvi, and James Glass. 2017b. [Eval-
uating layers of representation in neural machine
translation on part-of-speech and semantic tagging
tasks](#). In *Proceedings of the Eighth International
Joint Conference on Natural Language Processing
(Volume 1: Long Papers)*, pages 1–10, Taipei, Taiwan.
Asian Federation of Natural Language Processing.

Tom B. Brown, Benjamin Mann, Nick Ryder, Melanie
Subbiah, Jared Kaplan, Prafulla Dhariwal, Arvind
Neelakantan, Pranav Shyam, Girish Sastry, Amanda
Askell, Sandhini Agarwal, Ariel Herbert-Voss,
Gretchen Krueger, Tom Henighan, Rewon Child,
Aditya Ramesh, Daniel M. Ziegler, Jeffrey Wu,
Clemens Winter, Christopher Hesse, Mark Chen, Eric
Sigler, Mateusz Litwin, Scott Gray, Benjamin Chess,
Jack Clark, Christopher Berner, Sam McCandlish,
Alec Radford, Ilya Sutskever, and Dario Amodei.
2020. [Language models are few-shot learners](#). In *Ad-
vances in Neural Information Processing Systems 33:
Annual Conference on Neural Information Process-
ing Systems 2020, NeurIPS 2020, December 6-12,
2020, virtual*.

Rich Caruana. 1997. [Multitask learning](#). *Mach. Learn.*,
28(1):41–75.

Aakanksha Chowdhery, Sharan Narang, Jacob Devlin,
Maarten Bosma, Gaurav Mishra, Adam Roberts,
Paul Barham, Hyung Won Chung, Charles Sutton,
Sebastian Gehrmann, Parker Schuh, Kensen Shi,
Sasha Tsvyashchenko, Joshua Maynez, Abhishek
Rao, Parker Barnes, Yi Tay, Noam Shazeer, Vin-
odkumar Prabhakaran, Emily Reif, Nan Du, Ben
Hutchinson, Reiner Pope, James Bradbury, Jacob
Austin, Michael Isard, Guy Gur-Ari, Pengcheng Yin,
Toju Duke, Anselm Levskaya, Sanjay Ghemawat,
Sunipa Dev, Henryk Michalewski, Xavier Garcia,
Vedant Misra, Kevin Robinson, Liam Fedus, Denny
Zhou, Daphne Ippolito, David Luan, Hyeontaek Lim,
Barret Zoph, Alexander Spiridonov, Ryan Sepassi,
David Dohan, Shivani Agrawal, Mark Omernick, An-
drew M. Dai, Thanumalayan Sankaranarayanan Pil-
lai, Marie Pellat, Aitor Lewkowycz, Erica Moreira,
Rewon Child, Aleksandr Polozov, Katherine Lee,
Zongwei Zhou, Xuezhi Wang, Brennan Saeta, Mark
Diaz, Orhan Firat, Michele Catasta, Jason Wei, Kathy
Meier-Hellstern, Douglas Eck, Jeff Dean, Slav Petrov,
and Noah Fiedel. 2023. [Palm: Scaling language mod-
eling with pathways](#). *J. Mach. Learn. Res.*, 24:240:1–
240:113.

Hyung Won Chung, Le Hou, Shayne Longpre, Barret
Zoph, Yi Tay, William Fedus, Yunxuan Li, Xuezhi
Wang, Mostafa Dehghani, Siddhartha Brahma, Al-
bert Webson, Shixiang Shane Gu, Zhuyun Dai,

809	Colin Raffel, Noam Shazeer, Adam Roberts, Katherine Lee, Sharan Narang, Michael Matena, Yanqi Zhou, Wei Li, and Peter J. Liu. 2020. Exploring the limits of transfer learning with a unified text-to-text transformer . <i>J. Mach. Learn. Res.</i> , 21:140:1–140:67.	
810		
811		
812		
813		
814	Maithra Raghu, Justin Gilmer, Jason Yosinski, and Jascha Sohl-Dickstein. 2017. SVCCA: singular vector canonical correlation analysis for deep learning dynamics and interpretability . In <i>Advances in Neural Information Processing Systems 30: Annual Conference on Neural Information Processing Systems 2017, December 4-9, 2017, Long Beach, CA, USA</i> , pages 6076–6085.	
815		
816		
817		
818		
819		
820		
821		
822	Anna Rogers, Olga Kovaleva, and Anna Rumshisky. 2020. A primer in BERTology: What we know about how BERT works . <i>Transactions of the Association for Computational Linguistics</i> , 8:842–866.	
823		
824		
825		
826	Victor Sanh, Albert Webson, Colin Raffel, Stephen H. Bach, Lintang Sutawika, Zaid Alyafeai, Antoine Chaffin, Arnaud Stiegler, Arun Raja, Manan Dey, M Saiful Bari, Canwen Xu, Urmish Thakker, Shanya Sharma Sharma, Eliza Szczechla, Taewoon Kim, Gunjan Chhablani, Nihal V. Nayak, Debajyoti Datta, Jonathan Chang, Mike Tian-Jian Jiang, Han Wang, Matteo Manica, Sheng Shen, Zheng Xin Yong, Harshit Pandey, Rachel Bawden, Thomas Wang, Trishala Neeraj, Jos Rozen, Abheesht Sharma, Andrea Santilli, Thibault Févry, Jason Alan Fries, Ryan Teehan, Teven Le Scao, Stella Biderman, Leo Gao, Thomas Wolf, and Alexander M. Rush. 2022. Multi-task prompted training enables zero-shot task generalization . In <i>The Tenth International Conference on Learning Representations, ICLR 2022, Virtual Event, April 25-29, 2022</i> . OpenReview.net.	
827		
828		
829		
830		
831		
832		
833		
834		
835		
836		
837		
838		
839		
840		
841		
842		
843	Mirac Suzgun, Nathan Scales, Nathanael Schärli, Sebastian Gehrmann, Yi Tay, Hyung Won Chung, Aakanksha Chowdhery, Quoc V Le, Ed H Chi, Denny Zhou, , and Jason Wei. 2022. Challenging big-bench tasks and whether chain-of-thought can solve them . <i>arXiv preprint arXiv:2210.09261</i> .	
844		
845		
846		
847		
848		
849	Hugo Touvron, Louis Martin, Kevin Stone, Peter Albert, Amjad Almahairi, Yasmine Babaei, Nikolay Bashlykov, Soumya Batra, Prajjwal Bhargava, Shruti Bhosale, Dan Bikel, Lukas Blecher, Cristian Canton Ferrer, Moya Chen, Guillem Cucurull, David Esiobu, Jude Fernandes, Jeremy Fu, Wenyin Fu, Brian Fuller, Cynthia Gao, Vedanuj Goswami, Naman Goyal, Anthony Hartshorn, Saghar Hosseini, Rui Hou, Hakan Inan, Marcin Kardas, Viktor Kerkez, Madian Khabsa, Isabel Kloumann, Artem Korenev, Punit Singh Koura, Marie-Anne Lachaux, Thibaut Lavril, Jenya Lee, Diana Liskovich, Yinghai Lu, Yuning Mao, Xavier Martinet, Todor Mihaylov, Pushkar Mishra, Igor Molybog, Yixin Nie, Andrew Poulton, Jeremy Reizenstein, Rashi Rungta, Kalyan Saladi, Alan Schelten, Ruan Silva, Eric Michael Smith, Ranjan Subramanian, Xiaoqing Ellen Tan, Binh Tang, Ross Taylor, Adina Williams, Jian Xiang Kuan, Puxin Xu, Zheng Yan, Iliyan Zarov, Yuchen Zhang, Angela Fan,	
850		
851		
852		
853		
854		
855		
856		
857		
858		
859		
860		
861		
862		
863		
864		
865		
866		
867		
	Melanie Kambadur, Sharan Narang, Aurelien Rodriguez, Robert Stojnic, Sergey Edunov, and Thomas Scialom. 2023. Llama 2: Open foundation and fine-tuned chat models . <i>Preprint</i> , arXiv:2307.09288.	868
		869
		870
		871
	Laurens Van der Maaten and Geoffrey Hinton. 2008. Visualizing data using t-sne . <i>Journal of machine learning research</i> , 9(11).	872
		873
		874
	Liang Wang, Nan Yang, Xiaolong Huang, Linjun Yang, Rangan Majumder, and Furu Wei. 2024. Improving text embeddings with large language models . <i>Preprint</i> , arXiv:2401.00368.	875
		876
		877
		878
	Jason Wei, Maarten Bosma, Vincent Y. Zhao, Kelvin Guu, Adams Wei Yu, Brian Lester, Nan Du, Andrew M. Dai, and Quoc V. Le. 2022a. Finetuned language models are zero-shot learners . In <i>The Tenth International Conference on Learning Representations, ICLR 2022, Virtual Event, April 25-29, 2022</i> . OpenReview.net.	879
		880
		881
		882
		883
		884
		885
	Jason Wei, Yi Tay, Rishi Bommasani, Colin Raffel, Barret Zoph, Sebastian Borgeaud, Dani Yogatama, Maarten Bosma, Denny Zhou, Donald Metzler, Ed H. Chi, Tatsunori Hashimoto, Oriol Vinyals, Percy Liang, Jeff Dean, and William Fedus. 2022b. Emergent abilities of large language models . <i>Trans. Mach. Learn. Res.</i> , 2022.	886
		887
		888
		889
		890
		891
		892
	Thomas Wolf, Lysandre Debut, Victor Sanh, Julien Chaumond, Clement Delangue, Anthony Moi, Pierric Cistac, Tim Rault, Remi Louf, Morgan Funtowicz, Joe Davison, Sam Shleifer, Patrick von Platen, Clara Ma, Yacine Jernite, Julien Plu, Canwen Xu, Teven Le Scao, Sylvain Gugger, Mariama Drame, Quentin Lhoest, and Alexander Rush. 2020. Transformers: State-of-the-art natural language processing . In <i>Proceedings of the 2020 Conference on Empirical Methods in Natural Language Processing: System Demonstrations</i> , pages 38–45, Online. Association for Computational Linguistics.	893
		894
		895
		896
		897
		898
		899
		900
		901
		902
		903
		904
	Zheng Zhao, Yftah Ziser, and Shay Cohen. 2022. Understanding domain learning in language models through subpopulation analysis . In <i>Proceedings of the Fifth BlackboxNLP Workshop on Analyzing and Interpreting Neural Networks for NLP</i> , pages 192–209, Abu Dhabi, United Arab Emirates (Hybrid). Association for Computational Linguistics.	905
		906
		907
		908
		909
		910
		911
	Zheng Zhao, Yftah Ziser, Bonnie Webber, and Shay Cohen. 2023. A joint matrix factorization analysis of multilingual representations . In <i>Findings of the Association for Computational Linguistics: EMNLP 2023</i> , pages 12764–12783, Singapore. Association for Computational Linguistics.	912
		913
		914
		915
		916
		917
	Yaowei Zheng, Richong Zhang, Junhao Zhang, Yanhan Ye, Zheyang Luo, and Yongqiang Ma. 2024. Llamafactory: Unified efficient fine-tuning of 100+ language models . <i>arXiv preprint arXiv:2403.13372</i> .	918
		919
		920
		921

A Dataset Details

This appendix provides a detailed overview of the datasets used in this study. We followed Wei et al. (2022a) and organized all tasks into the following task clusters:

- **Closed-book Question Answering (QA)** requires models to answer questions about the world without direct access to the answer-containing information.
- **Commonsense Reasoning** tests the capacity for physical or scientific reasoning infused with common sense.
- **Coreference Resolution** identifies expressions referring to the same entity within a given text.
- **Natural Language Inference (NLI)** focuses on the relationship between two sentences, typically evaluating if the second sentence is true, false, or possibly true based on the first sentence.
- **Paraphrase Detection** involves evaluating if two sentences have the same meaning. While it can be considered a form of bidirectional entailment, it remains distinct from NLI in academic contexts.
- **Reading Comprehension** assesses the ability to answer questions based on a given passage containing the necessary information.
- **Reading Comprehension with Commonsense** merges the tasks of reading comprehension and commonsense reasoning.
- **Sentiment Analysis** is a traditional NLP task that determines whether a text expresses a positive or negative sentiment.
- **Struct-to-Text** involves generating natural language descriptions from structured data.
- **Translation** is the task of translating text from one language to another.
- **Summarization** involves creating concise summaries from longer texts.
- **Unseen** clusters uses the original miscellaneous task cluster from Wei et al. (2022a) which includes:

1. Conversational question-answering; 965
2. Evaluating context-sentence word meanings; 966
3. Linguistic acceptability; 968
4. Math questions; 969
5. Question classification. 970

We provide tasks contained in each cluster in Table 1. 971

B Additional Results 973

B.1 Results on Model Evaluation 974

We provide the results on all control models and instruction-tuned Llama 2-SFT in Table 3 (for natural language understanding tasks) and Table 4 (for natural language generation tasks). To further evaluate the validness of our instruction tuning, we also benchmark our models on two popular benchmark datasets: MMLU (Hendrycks et al., 2021) and BBH (Suzgun et al., 2022). We provide results in Table 2. We can see that Llama 2-SFT outperforms Llama 2 on both of these benchmarks. 975

B.2 Results on Analysis 985

Here we provide additional results on our analysis. We provide the distribution of CKA similarities for all layers by tasks clusters in Figure 8 and 9. We also provide Pearson correlation results between the CKA similarities for all tasks and their data size among all layers in Figure 10. Lastly, we provide the t-SNE visualizations of representations in different layers of Llama 2 in Figure 11. We provide the same visualizations for Llama 2-SFT in Figure 12. 986

Task Cluster	Dataset	Task Cluster	Dataset
Natural language inference	ANLI CB MNLI QNLI SNLI WNLI RTE	Reading comprehension	BoolQ DROP MultiRC OBQA SQuADv1 SQuADv2
Commonsense reasoning	COPA HellaSwag PiQA StoryCloze	Sentiment analysis	IMDB Sentiment140 SST-2 Yelp
Closed-book QA	ARC NQ TriviaQA	Paraphrase detection	MRPC QQP Paws Wiki STS-B
Coreference resolution	DPR Winogrande WSC273	Reading comprehension with commonsense	CosmosQA ReCoRD
Struct to text	CommonGen DART E2ENLG WebNLG	Translation	En-Fr from WMT'14 WMT'16 En-Es from Paracrawl
Summarization	AESLC CNN-DM Gigaword MultiNews Newsroom Samsun XSum AG News Opinion Abstracts - Rotten Tomatoes Opinion Abstracts - iDebate Wikilingua English	Unseen	CoQA QuAC WiC TREC CoLA Math questions

Table 1: Dataset details grouped by task clusters. For WMT'16, we include En-De, En-Tr, En-Cs, En-Fi, En-Ro, and En-Ru translation pairs. For all details about each dataset including the data set size, please refer to [Wei et al. \(2022a\)](#).

	MMLU	BBH
Llama 2	41.25	32.82
Llama 2-SFT	47.81	37.49

Table 2: Results for Llama 2 and Llama 2-SFT on MMLU and BBH. We use a 0-shot evaluation for MMLU to assess our models. For BBH, we follow the default evaluation protocol and use a 3-shot evaluation.

Dataset	Metric	Result	
		Llama 2-SFT	Control Model
Natural Language Inference			
ANLI (r1)	Accuracy	51.87	54.45
ANLI (r2)	Accuracy	49.45	55.85
ANLI (r3)	Accuracy	47.48	54.14
CB	Accuracy	49.59	83.17
MNLI (matched)	Accuracy	87.25	88.64
MNLI (mismatched)	Accuracy	87.72	89.41
QNLI	Accuracy	83.00	86.46
SNLI	Accuracy	82.96	84.06
WNLI	Accuracy	71.22	69.64
RTE	Accuracy	81.52	81.21
Reading Comprehension			
BoolQ	Accuracy	83.53	88.18
DROP	F1	44.42	52.05
MultiRC	F1	72.19	73.92
OBQA	Accuracy	64.92	65.37
SQuADv1	F1	73.91	74.24
SQuADv2	F1	22.75	23.55
Commonsense Reasoning			
COPA	Accuracy	83.56	76.97
HellaSwag	Accuracy	71.43	73.49
PiQA	Accuracy	78.21	78.43
StoryCloze	Accuracy	85.81	84.82
Sentiment Analysis			
IMDB	Accuracy	72.06	74.54
Sentiment140	Accuracy	45.52	44.53
SST-2	Accuracy	79.14	79.03
Yelp	Accuracy	74.35	74.40
Closed-book QA			
ARC (Challenge)	Accuracy	59.09	52.83
ARC (Easy)	Accuracy	67.18	65.72
TriviaQA	Accuracy	59.00	59.26
NQ	Accuracy	28.79	31.18
Paraphrase Detection			
MRPC	Accuracy	78.35	84.73
QQP	Accuracy	84.91	87.37
PAWS Wiki	Accuracy	91.77	94.15
STS-B	Accuracy	47.46	51.20
Coreference Resolution			
DPR	Accuracy	85.12	72.53
Winogrande	Accuracy	69.68	69.93
WSC273	Accuracy	55.78	47.24
Read. Comp. w/ Commonsense			
CosmosQA	Accuracy	66.60	69.36
ReCoRD	Accuracy	85.13	85.78
Unseen			
CoQA	Accuracy	66.60	73.93
QuAC	Accuracy	18.29	33.99
WiC	Accuracy	56.47	70.77
TREC	Accuracy	57.05	80.25
CoLA	Accuracy	34.85	70.91
Math Questions	Accuracy	4.43	35.50

Table 3: Performance metrics grouped by natural language understanding task clusters for Llama 2-SFT and control models (Llama 2 model individually fine-tuned on each task). “Read. Comp. w/ Commonsense” denotes reading comprehension with commonsense.

Dataset	Metric	Result	
		Llama 2-SFT	Control Model
Struct-to-Text			
CommonGen	ROUGE-L	45.92	46.52
DART	ROUGE-L	55.46	57.28
E2ENLG	ROUGE-L	50.17	50.96
WebNLG	ROUGE-L	62.92	65.22
Translation			
WMT'14 En-Fr	BLEU	59.30	59.29
WMT'16 En-De	BLEU	56.84	57.45
WMT'16 En-Tr	BLEU	39.41	43.58
WMT'16 En-Cs	BLEU	46.92	47.21
WMT'16 En-Fi	BLEU	48.57	50.28
WMT'16 En-Ro	BLEU	56.03	57.70
WMT'16 En-Ru	BLEU	51.41	52.12
ParaCrawl En-Es	BLEU	54.76	56.39
Summarization			
AESLC	ROUGE-L	29.98	31.68
CNN-DM	ROUGE-L	17.38	19.59
Gigaword	ROUGE-L	28.69	30.22
MultiNews	ROUGE-L	15.17	16.61
Newsroom	ROUGE-L	18.95	22.43
Samsun	ROUGE-L	36.36	37.72
XSum	ROUGE-L	25.51	29.57
AG News	ROUGE-L	77.26	80.99
Opinion Abstracts - Rotten Tomatoes	ROUGE-L	19.36	21.70
Opinion Abstracts - iDebate	ROUGE-L	18.90	23.14
Wikilingua English	ROUGE-L	30.22	32.18

Table 4: Performance metrics grouped by natural language generation task clusters for Llama 2-SFT and control models (Llama 2 model individually fine-tuned on each task).

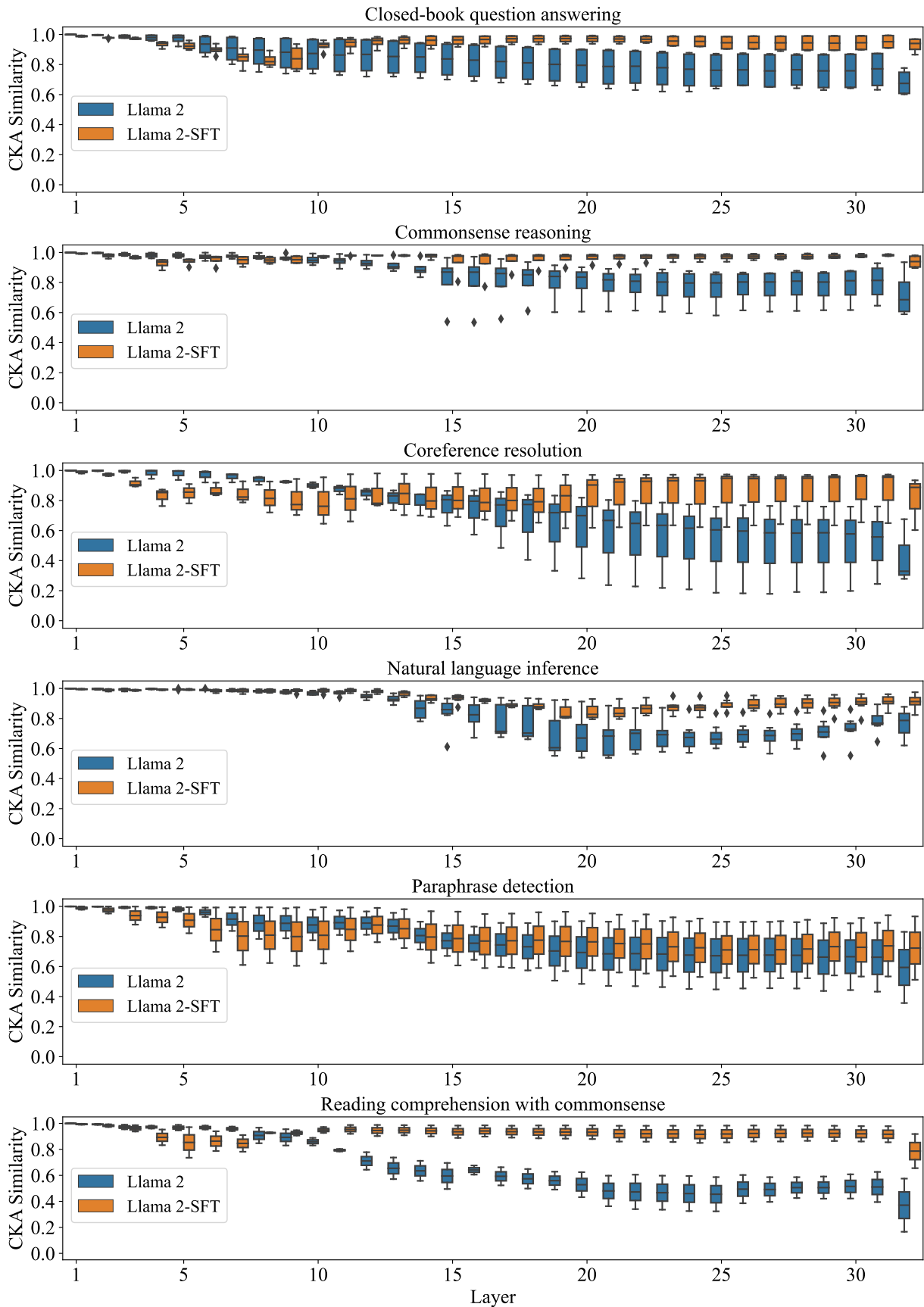


Figure 8: Distribution of CKA similarities across all layers for the pre-trained Llama 2 model and the instruction-tuned Llama 2-SFT model, grouped by different task clusters.

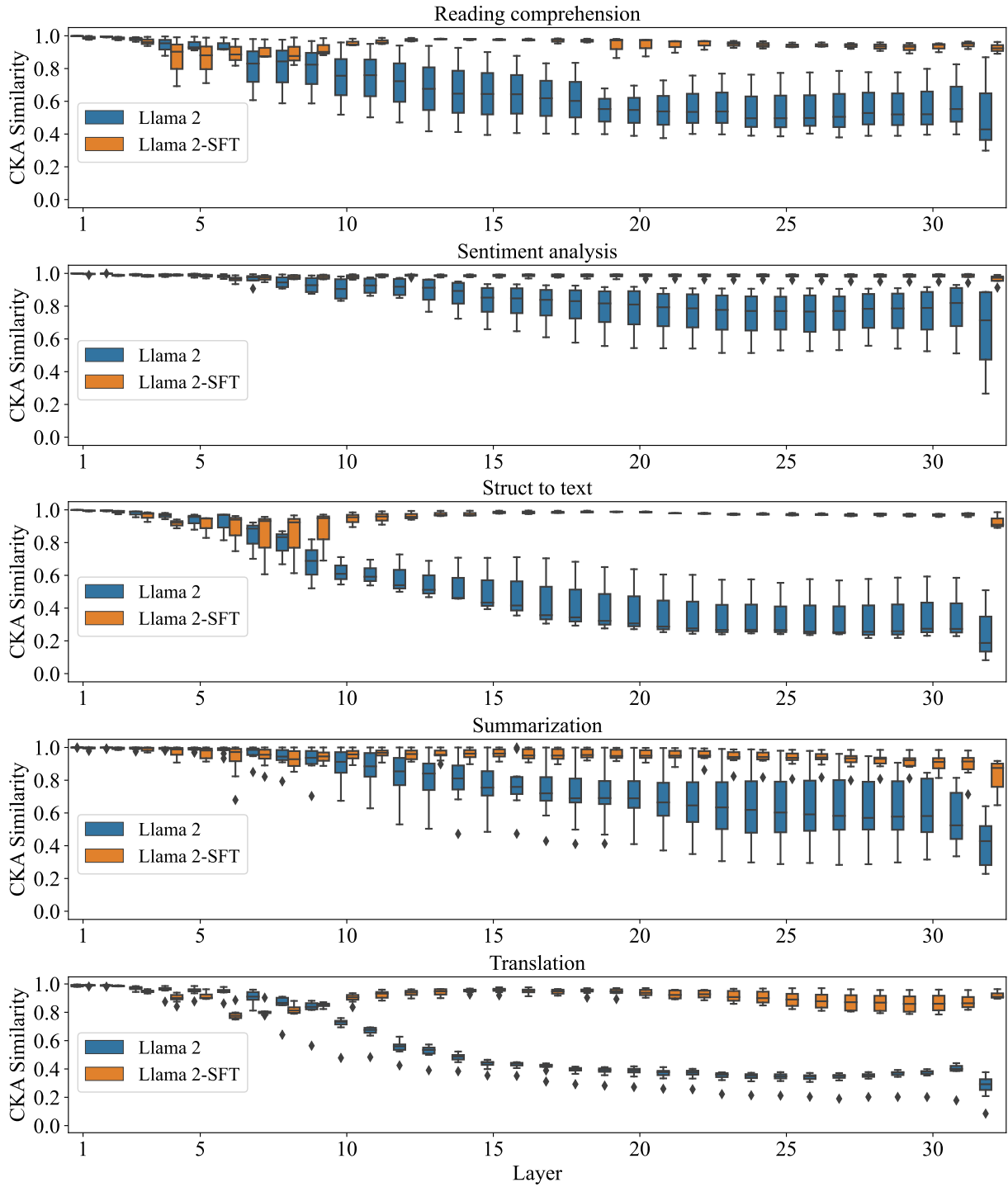


Figure 9: Distribution of CKA similarities across all layers for the pre-trained Llama 2 model and the instruction-tuned Llama 2-SFT model, grouped by different task clusters.

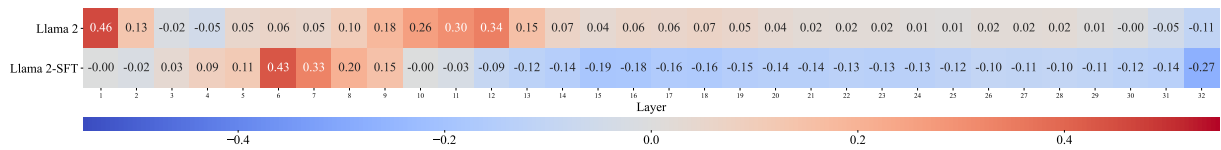


Figure 10: Pearson correlation results between the CKA similarities for all tasks and their data size among all layers.

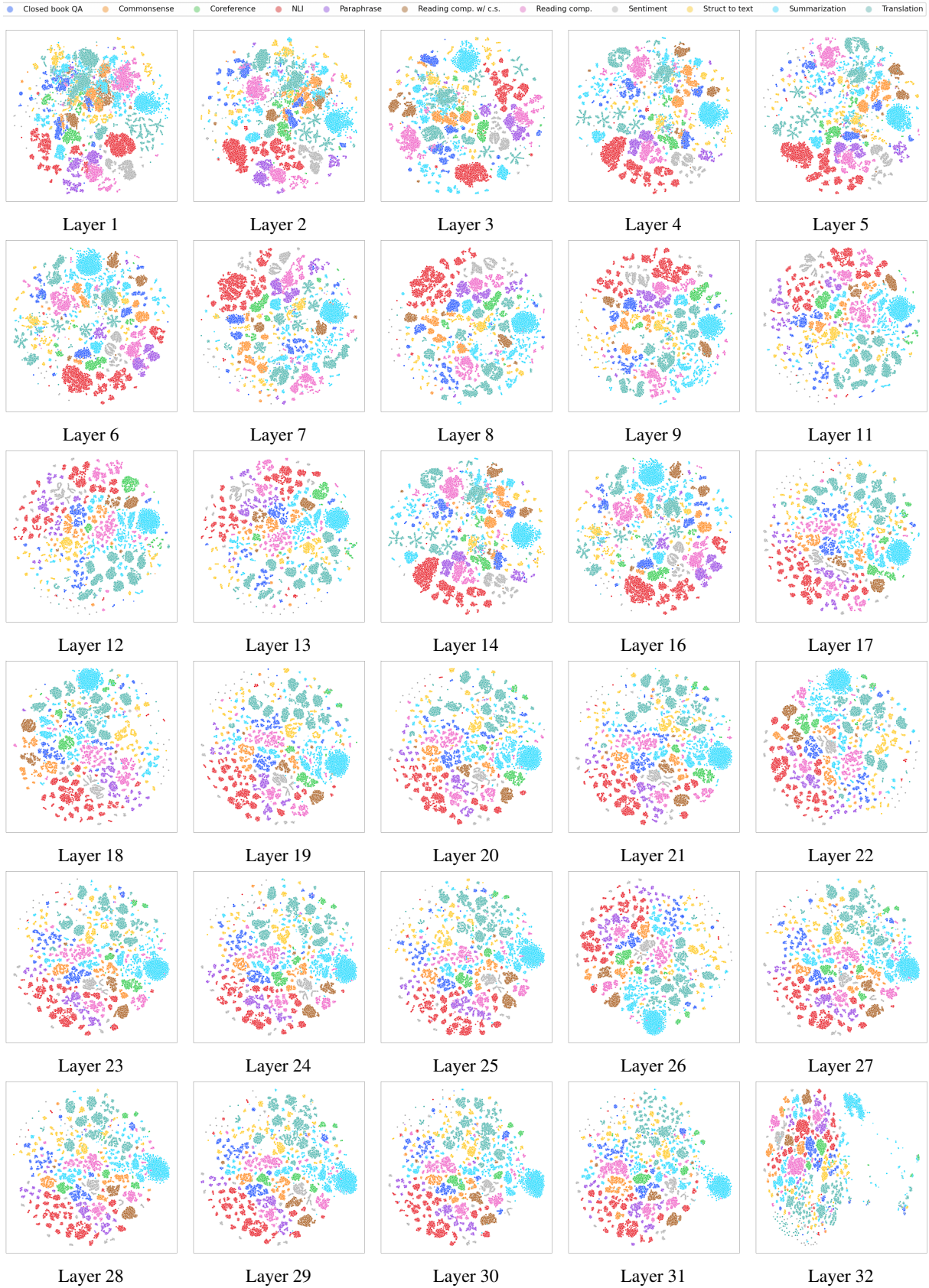


Figure 11: t-SNE visualizations of the representations for each task cluster in different layers of the pre-trained Llama 2 model. Each subplot presents the t-SNE projection of the representations, color-coded by task cluster, for a specific layer of the respective model. “Reading comp.” denotes reading comprehension tasks, and “reading comp. w/ c.s.” denotes reading comprehension tasks with commonsense reasoning. We omit layer 10 and 15 to fit in one page and as we have provided them earlier.

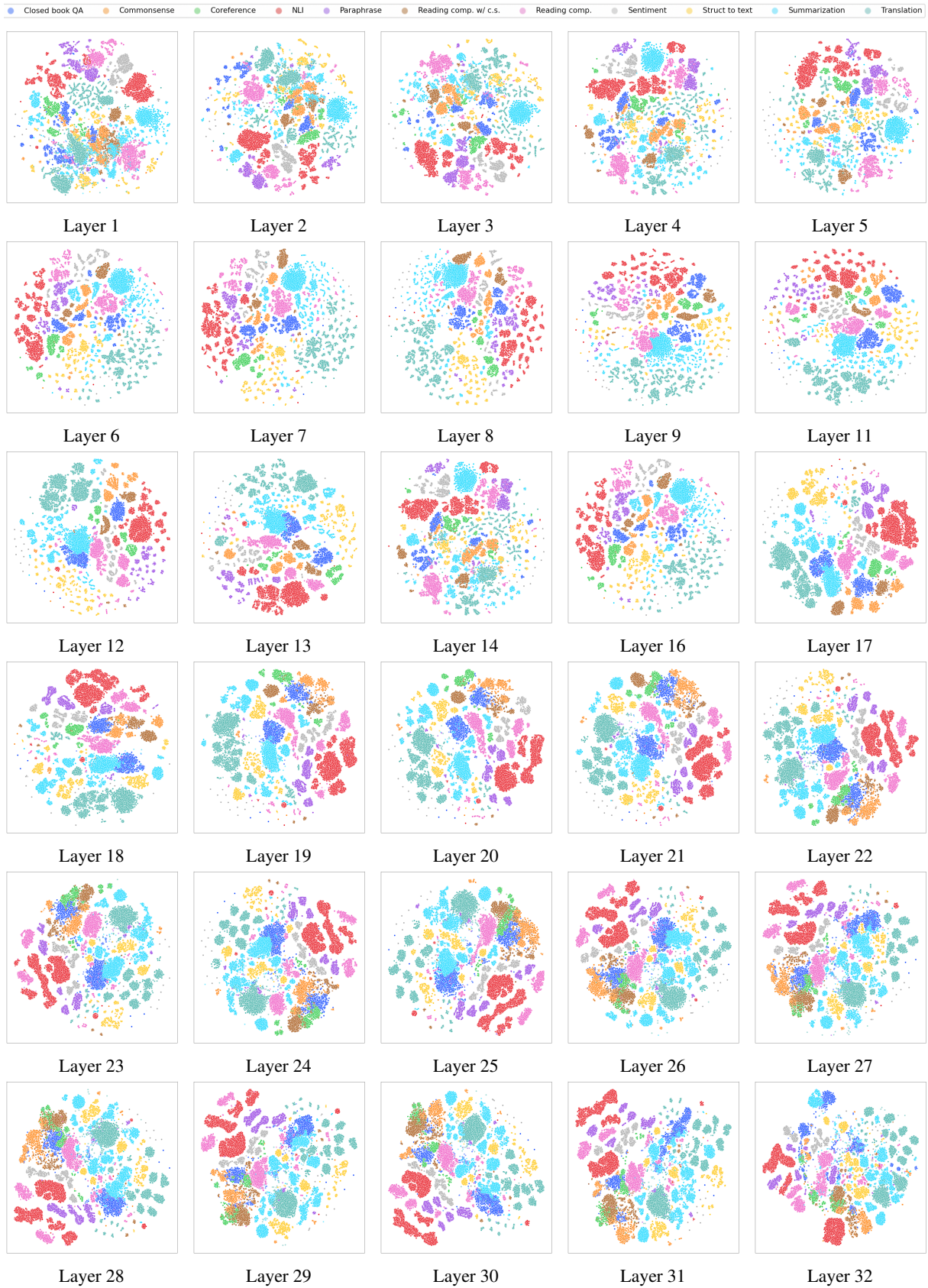


Figure 12: t-SNE visualizations of the representations for each task cluster in different layers of the instruction-tuned Llama 2-SFT model. Each subplot presents the t-SNE projection of the representations, color-coded by task cluster, for a specific layer of the respective model. “Reading comp.” denotes reading comprehension tasks, and “reading comp. w/ c.s.” denotes reading comprehension tasks with commonsense reasoning. We omit layer 10 and 15 to fit in one page and as we have provided them earlier.